AD-A057 254 PACIFIC-SIERRA RESEARCH CORP SANTA MONICA CALIF F/G 20/14
ANALYSIS OF ELECTRON DENSITY-PROFILES IN THE LOWER IONOSPHERE.(U)
MAR 78 E C FIELD, M LEWINSTEIN F19628-77-C-0231
UNCLASSIFIED PSR-801 RADC-TR-78-67 NL

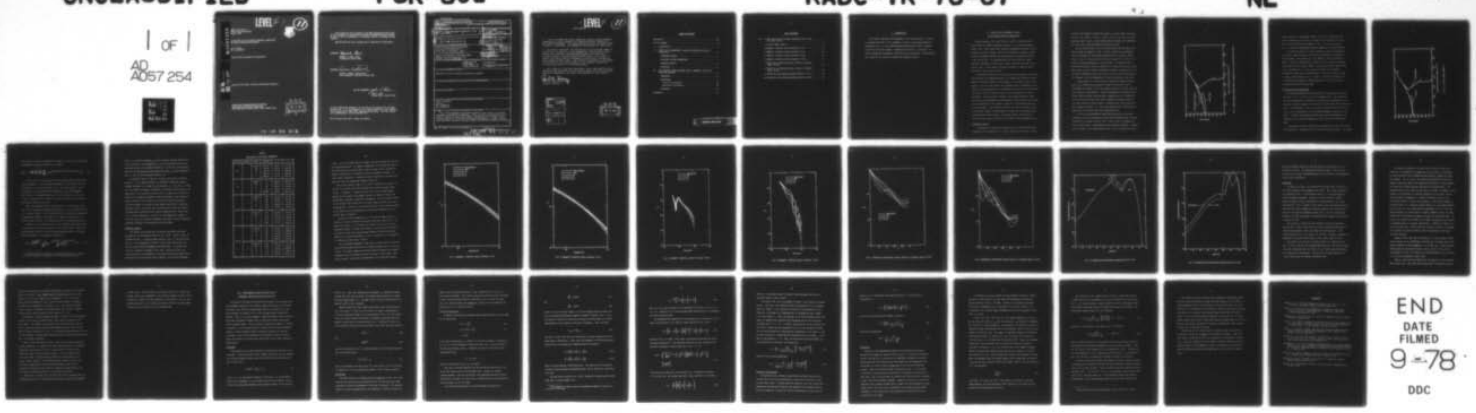

END
DATE FILMED
9-78
DDC

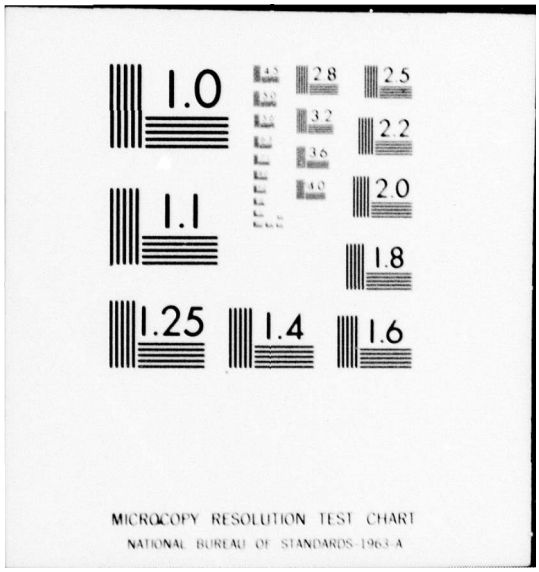
1.0
1.1
1.25
1.4
1.6
1.8
2.0
2.2
2.5
2.8
3.2
3.6
4.0
MICROCOPY RESOLUTION TEST CHART
NATIONAL BUREAU OF STANDARDS-1963-A

AD A057254

LEVEL II 8

RADC-TR-78-67
Final Technical Report
March 1978

ANALYSIS OF ELECTRON DENSITY-PROFILES IN THE LOWER IONOSPHERE

E.C. Field
M. Lewinstein

Pacific-Sierra Research Corporation

AD No.____
DDC FILE COPY

Approved for public release; distribution unlimited

ROME AIR DEVELOPMENT CENTER
AIR FORCE SYSTEMS COMMAND
GRIFFISS AIR FORCE BASE, NEW YORK 13441

DDC
RECEIVED
AUG 9 1978
D

78 08 04 012

This report has been reviewed by the RADC Information Office (OI) and is releasable to the National Technical Information Service (NTIS). At NTIS it will be releasable to the general public, including foreign nations.

RADC-TR-78-67 has been reviewed and is approved for publication.

APPROVED: Edward A. Lewis

EDWARD A. LEWIS, Chief
Propagation Branch (EEP)

APPROVED: Allan C. Schell

ALLAN C. SCHELL, Acting Chief
Electromagnetic Sciences Division (EE)

FOR THE COMMANDER: John P. Huss

JOHN P. HUSS
Acting Chief, Plans Office

If your address has changed or if you wish to be removed from the RADC mailing list, or if the addressee is no longer employed by your organization, please notify RADC (EEP) Hanscom AFB MA 01731. This will assist us in maintaining a current mailing list.

Do not return this copy. Retain or destroy.

UNCLASSIFIED

SECURITY CLASSIFICATION OF THIS PAGE (When Data Entered)

REPORT DOCUMENTATION PAGE

READ INSTRUCTIONS BEFORE COMPLETING FORM

1. REPORT NUMBER: RADC-TR-78-67	2. GOVT ACCESSION NO.
3. RECIPIENT'S CATALOG NUMBER	
4. TITLE (and Subtitle): ANALYSIS OF ELECTRON DENSITY-PROFILES IN THE LOWER IONOSPHERE	5. TYPE OF REPORT & PERIOD COVERED: Final Report, 1 Aug 77 -- 30 Nov 77
6. PERFORMING ORG. REPORT NUMBER: PSR-801	
7. AUTHOR(s): E. C. Field and M. Lewinstein	8. CONTRACT OR GRANT NUMBER(s): F19628-77-C-0231
9. PERFORMING ORGANIZATION NAME AND ADDRESS: Pacific-Sierra Research Corporation, 1456 Cloverfield Boulevard, Santa Monica, California 90404	10. PROGRAM ELEMENT, PROJECT, TASK AREA & WORK UNIT NUMBERS: 61102F 2304 J321 J3
11. CONTROLLING OFFICE NAME AND ADDRESS: Deputy for Electronic Technology (RADC), Hanscom AFB, Massachusetts 01731, Monitor: Paul A. Kossey/EEP	12. REPORT DATE: March 1978; 13. NUMBER OF PAGES: 39
14. MONITORING AGENCY NAME & ADDRESS (if different from Controlling Office): 40 p.	15. SECURITY CLASS. (of this report): UNCLASSIFIED
	15a. DECLASSIFICATION/DOWNGRADING SCHEDULE

16. DISTRIBUTION STATEMENT (of this Report)

Approved for public release; distribution unlimited.

17. DISTRIBUTION STATEMENT (of the abstract entered in Block 20, if different from Report)

18. SUPPLEMENTARY NOTES

19. KEY WORDS (Continue on reverse side if necessary and identify by block number)

lower ionosphere
C-layer
ELF propagation
VLF propagation

20. ABSTRACT (Continue on reverse side if necessary and identify by block number)

This report addresses two separate aspects of the effects of the lower ionosphere on ELF/VLF/LF propagation. First, full-wave calculations are performed to assess the effect of a ledge of ionization in the 55-km to 65-km altitude range (e.g., "C-layer") on long-path propagation. Second, relationships among wave frequency, incidence angle, and refraction heights are derived.

DD FORM 1 JAN 73 1473 EDITION OF 1 NOV 65 IS OBSOLETE

UNCLASSIFIED

SECURITY CLASSIFICATION OF THIS PAGE (When Data Entered)

78 08 04 012
407 486

LEVEL II

11

EVALUATION

1. I have reviewed the Final Report by Pacific Sierra Research Corporation, titled ANALYSIS OF ELECTRON DENSITY-PROFILES IN THE LOWER IONOSPHERE. The report describes work performed under contract to RADC/EEP, and represents the product of that work.

2. The report describes the effects of a low altitude ledge of ionization ("C-layer") on the propagation of ELF/VLF/LF radio waves; and, derives relationships between wave frequency, incidence angle, and reflection heights which can be used to deduce grazing incidence ionospheric reflectivity information from steep-incidence data. The research described in the report contributes to the understanding of the complex interaction of long radio waves in an ionized medium.

3. All aspects of the work contracted for by RADC/EEP have been completed and described in the subject report by Pacific Sierra Research Corporation, and meets the approval of this office.

Paul A. Kossey

Paul A. Kossey, EEP/x4265
Contract Monitor

ACCESSION for
NTIS White Section
DDC Buff Section
UNANNOUNCED
JUSTIFICATION
BY
DISTRIBUTION/AVAILABILITY CODES
DIST. AVAIL. and/or SPECIAL
A

DDC
RECEIVED
AUG 9 1978
D

TABLE OF CONTENTS

PRECEDING PAGE BLANK

LIST OF FIGURES

I. INTRODUCTION

This report comprises two independent, self-contained parts: Section II examines the effect of an ionospheric C-layer on long-range ELF/VLF/LF propagation; Sec. III, the relationships among incidence angle, frequency, and VLF/LF reflection heights. Subsections in both Sec. II and Sec. III present background discussions, derivations, and conclusions. Both sections can, therefore, be treated as essentially separate reports.

II. EFFECT OF AN IONOSPHERIC C-LAYER ON LONG-PATH ELF/VLF/LF PROPAGATION

Roughly speaking, the term "C-layer" refers to ionization that occurs below the normal ionospheric D-layer; i.e., below altitudes of around 65 km. Many authors have reported experimental evidence for the existence of such a C-layer. Most of this evidence is based on steep-incidence ionospheric-reflection data measured at frequencies between 15 kHz and 100 kHz. The characteristics of the C-layer are highly variable, depending on time of day, season, location, and phase of the sunspot cycle. There appear to be many locations or times at which a detectable C-layer does not exist.

As indicated above, most of the radio data pertaining to the C-layer were measured on transmission paths of no longer than 200 km to 300 km, where the incidence angle at the ionosphere is not greater than, say 60 degrees. For such short paths, the propagation may be adequately represented by the superposition of a ground wave plus first- and second-order "sky waves" that are reflected once or twice, respectively, from the ionosphere. At much greater distances, this simple plane-wave superposition becomes cumbersome, because numerous sky waves must be retained, and representation of the signal in terms of a few waveguide modes becomes preferable. This section calculates the effect of model C-layers on ELF/VLF/LF signals for pathlengths so large that the waveguide-mode representation should be used. We assume--without justification--that the C-layer exists over the entire length of the propagation path.

IONOSPHERIC MODELS

Our approach to assessing the sensitivity of long-path ELF/VLF/LF propagation to the presence of a C-layer consists of two steps. First,

we make field-strength calculations based on a nominal model ionosphere that does not exhibit a C-layer. Second, we alter this model by superimposing sample C-layers, recalculating field strengths, and comparing the results with those obtained for the nominal model.

For our nominal model, we use the DNA standard daytime model ionosphere (*Knapp and Schwartz, 1975*). Figure 1 shows the corresponding electron and positive ion-density height-profiles, N_e and N_+, respectively. Also, we assume the ion-collision frequency to be 1/40 of the electron collision-frequency at all altitudes. The masses of both positive and negative ions are assumed to be 65 AMU below 40 km, 40 AMU above 65 km, and are linearly interpolated between 40 km and 65 km. For the model ionospheres used in this report, the ions affect ELF propagation somewhat, but VLF propagation is totally dominated by electrons.

A large number of C-layer profiles, measured by numerous investigators, are reviewed and presented by Alpert (*1973*), Bain (*1974*), Krasnushkin and Federov (*1966*), and Risbeth and Garriot (*1969*), who also give extensive bibliographies. These experimentally determined layers exhibit widely varying characteristics, depending on local conditions at the time that the data were taken. Moreover, although consistent with low-frequency, steep-incidence, reflection data, these layers are not necessarily unique; i.e., some other assumed layer characteristics might also be consistent with the reflectivity data.

Of all the electron-density height-profiles given in the above references, the most pronounced C-layers had a maximum density of about 100 el/cm^3 at a height of about 55 km. Such a layer is assumed here, and is shown in Fig. 1 superimposed on the standard ionosphere. Throughout this report, the C-layer shown in Fig. 1 will be called the "Bain"

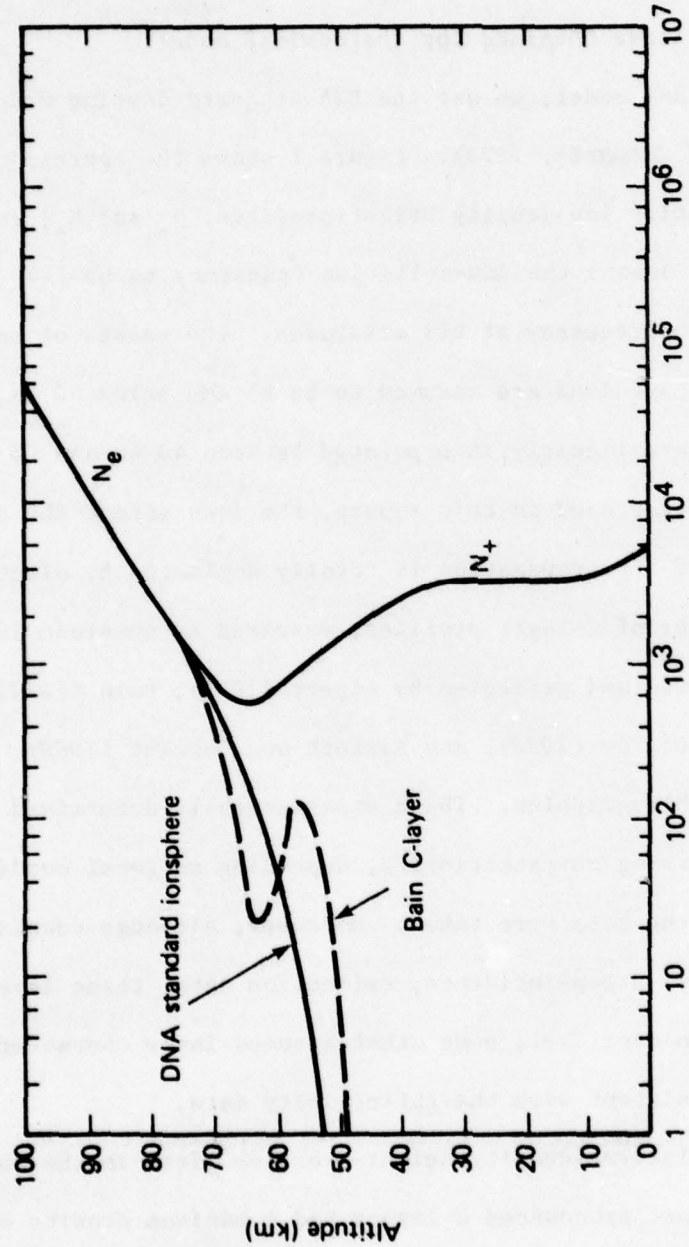

Fig. 1--DNA standard daytime model ionosphere and C-layer from Bain (1974)

C-layer because it corresponds closely to the most pronounced of the models considered by Bain (*1974*), although a very similar profile was also used by Krasnushkin and Federov (*1966*). The C-layer shown in Fig. 1 is based on measurements taken at summer noon in Great Britain.

To assess the effects of C-layer height on long-path propagation, we assume a ledge of density 100 el/cm^3 and thickness 6 km centered at three heights: 58 km (Model A), 55 km (Model B), and 61 km (Model C). Figure 2 shows the superposition of Model A on the standard ionosphere. Since Models B and C consist simply of moving the ledge of Model A down or up, respectively, by 3 km, they are not shown in the figures. Although the upper and lower boundaries of the C-layer ledge are shown as being totally abrupt in Fig. 2, they are "smeared" over about 1 km in performing the numerical calculations because of the 1-km height-resolution used for the input data.

EQUATIONS AND MODE PARAMETERS

The detailed equations describing ELF/VLF/LF propagation were given by Field, et al. (*1976*) and will not be repeated here. These equations are solved numerically, accounting for the vertical inhomogeneity of the ionosphere and the curvature of the earth, thus obtaining the results given below. The geomagnetic field of the earth is omitted from the calculation, which is permissible for the daytime propagation conditions considered. To define the notation and illustrate the key dependences, two equations for the spatial dependence of the fields are recapitulated below.

We consider vertically oriented VLF transmitters for which the fields are composed of a superposition of so-called TM waveguide modes. We express

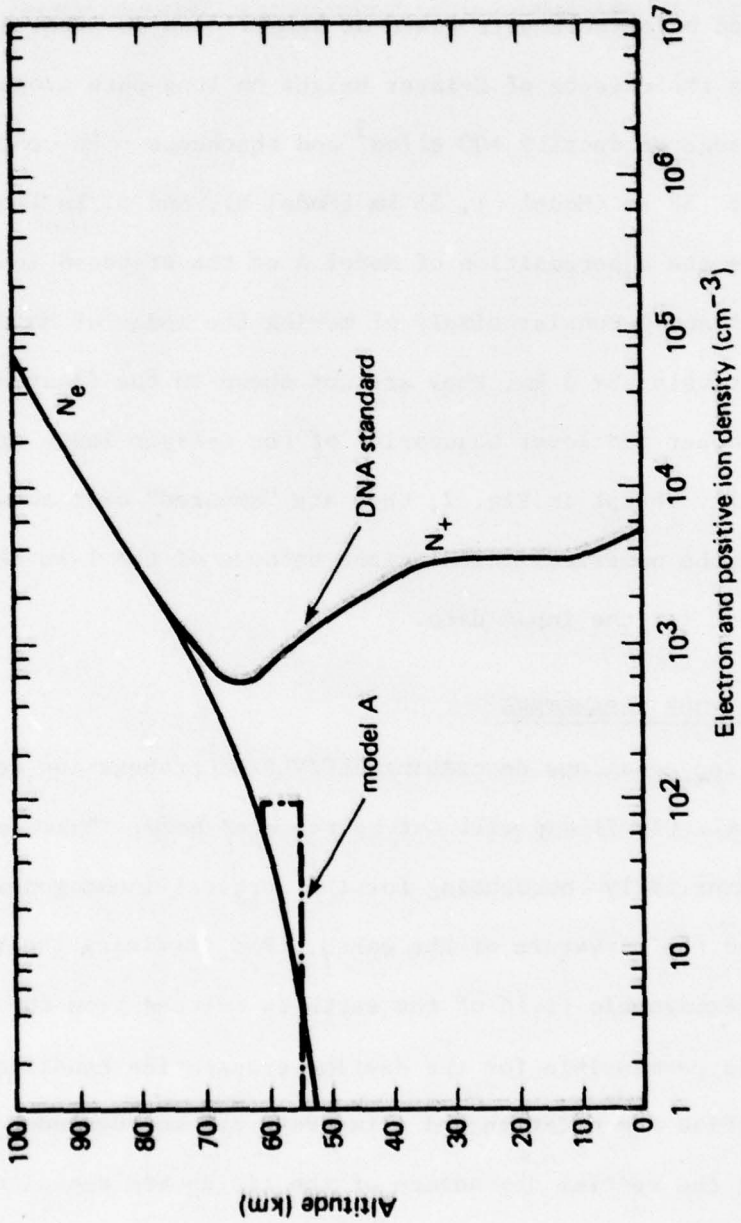

Fig. 2--C-layer ledge; Model A

the results in terms of the magnetic intensity, H, which is horizontally* oriented and is given by Field, et al. (*1976*):

$$H_{VLF} = iI\ell\sqrt{\frac{1}{\lambda d}}\sqrt{\frac{d/a}{\sin d/a}}\sum_{\alpha} \Lambda_\alpha S_\alpha^{\frac{1}{2}} e^{-\eta d/8.7\times10^{-6}} e^{-2\pi icd/\lambda v} e^{-\pi i/4} \text{ A/M.} \qquad (1)$$

In Eq. (1), $I\ell$ is the effective electric-dipole moment of the transmitting antenna; λ, the free-space wavelength; d, the distance from the transmitter; a, the earth's radius; and c, the vacuum speed of light. The quantity S_α is essentially the eigenvalue of the α^{th}-waveguide mode and must be computed numerically. At VLF, however, S_α turns out to have a magnitude close to unity, and the term $S_\alpha^{\frac{1}{2}}$ in Eq. (1) does not appreciably influence the field.

Thus, the magnitude of the vertical electric field depends on the state of the ionosphere through two parameters: Λ_α, the excitation factor for a vertical dipole; η, the attenuation rate in decibels per megameters of propagation (dB/Mm). The phase of the signal is governed by the relative phase velocity, v/c, which must also be determined numerically.

Contrary to the situation at VLF, an ELF transmitting antenna would be horizontally oriented and operated in the endfire mode to excite the quasi-TM mode, which is the only one that propagates well. The appropriate expression for the magnetic intensity is

$$H_{ELF} = \frac{iI\ell f}{120\pi}\sqrt{\frac{2\pi\mu_o}{c}}\ \frac{\Lambda_h}{\sqrt{\sigma_g c/v}} \cdot \frac{e^{-2\pi icd/\lambda v}\ e^{-\eta d/(8.7\times10^6)}}{\sqrt{a \sin d/a}} \text{ A/m} , \qquad (2)$$

*More precisely, we consider the azimuthal component, H_ϕ, where ϕ is the usual azimuthal coordinate in polar spherical coordinates.

where f is the wave frequency, σ_g is the effective ground conductivity in the vicinity of the transmitter, A_h is the excitation factor for a horizontal dipole in the endfire direction. As for VLF, the mode parameters to be calculated are the excitation factor, A_h, the attenuation rate, η, and the relative phase velocity, v/c.

As defined in Eqs. (1) and (2), A_α and A_h have units of inverse distance. In the idealized limit of a perfectly reflecting, sharply bounded ionosphere at a height H_o above ground, $A_\alpha \to 1/H_o$ and $A_h \to 1/2H_o$. Even for diffuse ionospheric boundaries (as treated in this report), the magnitudes of the excitation factors are of the same order as the reciprocal of the nominal ionospheric reflection heights. This definition differs from that often found in the literature, where the nominal reflection height is factored out and appears explicitly in equations analogous to Eqs. (1) and (2), and the excitation factors are treated as dimensionless quantities with order-of-magnitude unity rather than $1/H_o$. Stated differently, A_α in Eq. (1) corresponds very roughly to the ratio A_α/H_o often used in treatments that model the earth-ionosphere waveguide as having a well-defined reflection height.

NUMERICAL RESULTS

All results given below were calculated using PSR's full-wave propagation code described by Field, et al. (*1976*). Table 1 gives the attenuation rate, η, relative phase velocity, (v/c) -1, and excitation factor, A, for frequencies of 45 Hz, 75 Hz, 20 kHz, and 35 kHz, and the five daytime model ionospheres described above. A ground conductivity of 4 mhos/m is assumed in all cases. Results for only the lowest mode (No. 1) are shown for 45 Hz and 75 Hz, because higher-order ELF modes are well below the cutoff frequency of the earth-ionosphere

Table 1

CALCULATED ELF/VLF MODE PARAMETERS

Freq. (Hz)	Mode No.	Model	η (dB/Mm)	v/c - 1	Λ
45	1	Standard	-7.99×10^{-1}	-1.86×10^{-1}	9.23×10^{-6}
		Bain	-7.29×10^{-1}	-2.18×10^{-1}	9.95×10^{-6}
		A	-7.27×10^{-1}	-2.03×10^{-1}	9.62×10^{-6}
		B	-6.61×10^{-1}	-2.13×10^{-1}	9.84×10^{-6}
		C	-6.86×10^{-1}	-1.73×10^{-1}	8.93×10^{-6}
75	1	Standard	-1.14	-1.68×10^{-1}	9.00×10^{-6}
		Bain	-1.15	-2.03×10^{-1}	9.78×10^{-6}
		A	-1.07	-1.88×10^{-1}	9.46×10^{-6}
		B	-1.04	-1.99×10^{-1}	9.72×10^{-6}
		C	-9.34×10^{-1}	-1.60×10^{-1}	8.82×10^{-6}
20×10^{3}	1	Standard	-1.88	-1.64×10^{-3}	1.07×10^{-5}
		Bain	-3.26	-1.49×10^{-3}	1.13×10^{-5}
		A	-2.44	-1.41×10^{-3}	1.15×10^{-5}
		B	-2.78	-1.38×10^{-3}	1.16×10^{-5}
		C	-2.00	-1.55×10^{-3}	1.10×10^{-5}
	2	Standard	-7.97	1.07×10^{-2}	1.78×10^{-5}
		Bain	-14.71	1.06×10^{-2}	1.71×10^{-5}
		A	-11.29	1.16×10^{-2}	1.79×10^{-5}
		B	-12.77	1.15×10^{-2}	1.72×10^{-5}
		C	-8.83	1.11×10^{-2}	1.80×10^{-5}
35×10^{3}	1	Standard	-3.32	-3.54×10^{-3}	2.99×10^{-6}
		Bain	-6.39	-3.02×10^{-3}	4.99×10^{-6}
		A	-4.35	-3.14×10^{-3}	4.28×10^{-6}
		B	-5.31	-3.08×10^{-3}	4.60×10^{-6}
		C	-3.47	-3.39×10^{-3}	3.42×10^{-6}
	2	Standard	-4.53	8.49×10^{-4}	1.97×10^{-5}
		Bain	-12.05	1.13×10^{-3}	2.07×10^{-5}
		A	-7.31	1.32×10^{-3}	2.08×10^{-5}
		B	-9.10	1.25×10^{-3}	2.05×10^{-5}
		C	-5.14	1.05×10^{-3}	2.02×10^{-5}

cavity. For VLF (20 kHz) and LF (35 kHz), results are shown for the first two TM-waveguide modes. At higher frequencies, the attenuation rates of the various modes are nearly equal, with the result that a prohibitive number of modes must be retained to achieve reasonable accuracy. At these higher frequencies, a geometric-optical approach is generally more practical than the normal-mode approach used here.

The results shown in Table 1 are used in conjunction with Eqs. (1) and (2) to calculate the field-strength versus distance graphs shown in Figs. 3 through 6. Distances shorter than several hundred megameters are not shown on the graphs, because the number of modes used inadequately represents short-path propagation. Even the results shown do not achieve high accuracy until the path length exceeds, say, one or two megameters. Because we are interested solely in the relative values of the field for the various models, an arbitrary amplitude scale is used in Figs. 3 through 6.

To assist in the interpretation of the results shown in Figs. 3 through 6, we have calculated the normal reflection coefficient, $_{\perp\perp}R_{\perp\perp}$, versus the cosine, C, of the angle of incidence for each of the five ionospheric models. Because the concept of a reflection coefficient is not useful at ELF, where the wavelength greatly exceeds the distance between the earth and ionosphere, $|_{\perp\perp}R_{\perp\perp}|$ is given only for frequencies of 20 kHz and 35 kHz (Figs. 7 and 8).

As an additional diagnostic tool, Figs. 9 and 10 show the relative Joule-heating height-profile for the lowest waveguide mode at 75 Hz and 20 kHz. The figures compare the heating profiles between the standard ionosphere and the ionosphere having the "Bain" C-layer ledge. Note that the shape, rather than the magnitudes, of the heating profiles

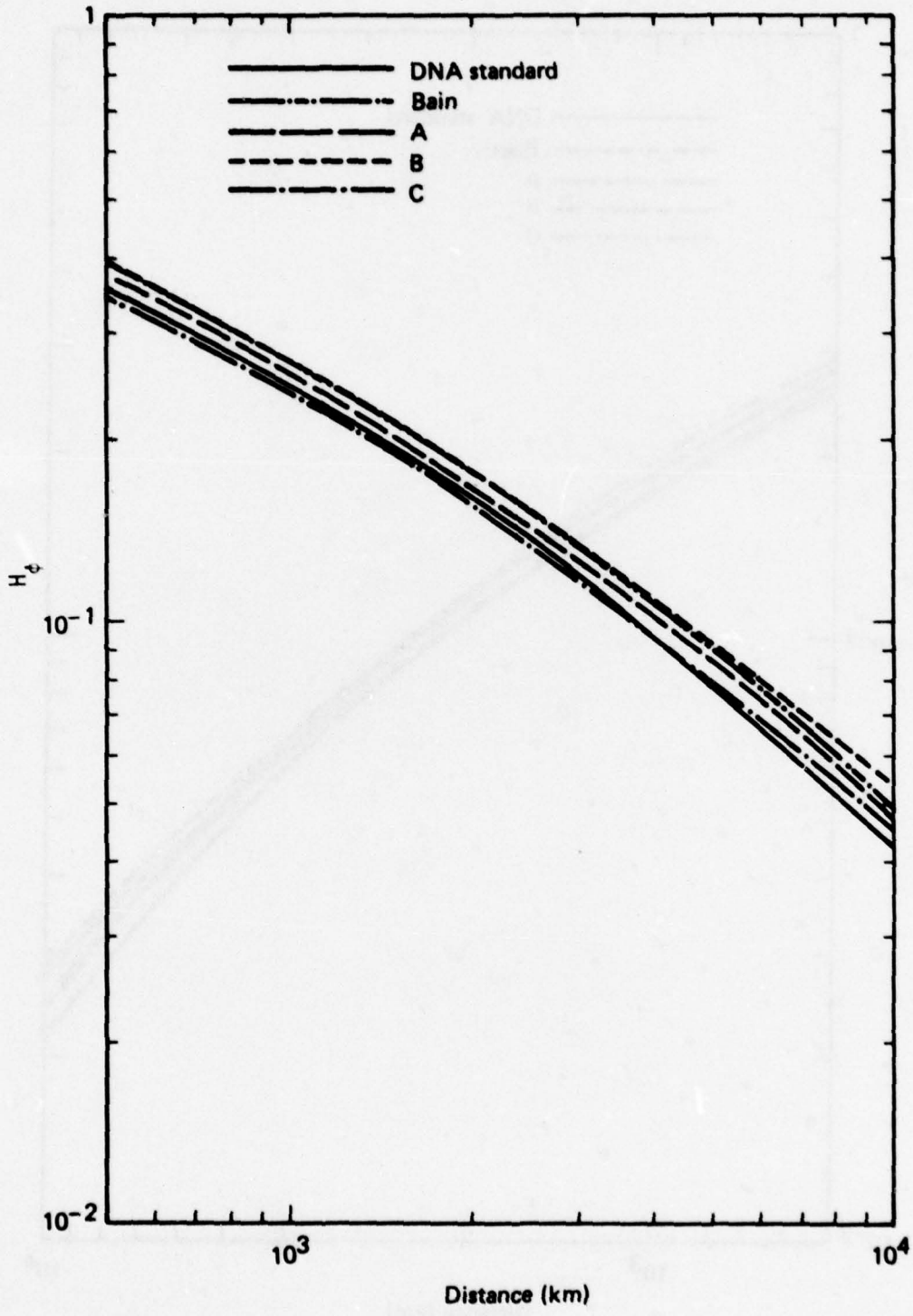

Fig. 3--Magnetic intensity versus distance; 45 Hz

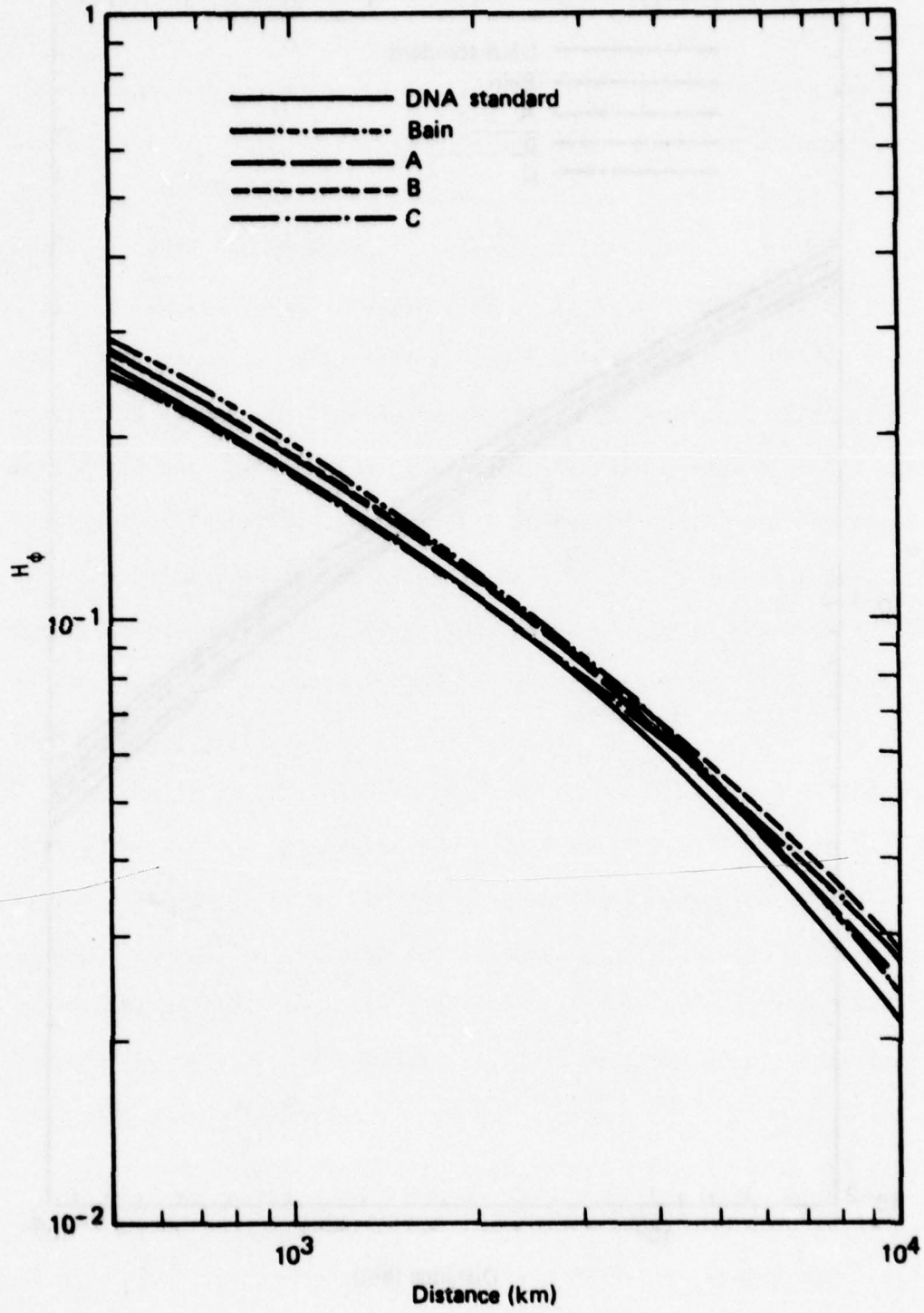

Fig. 4--Magnetic intensity versus distance; 75 Hz

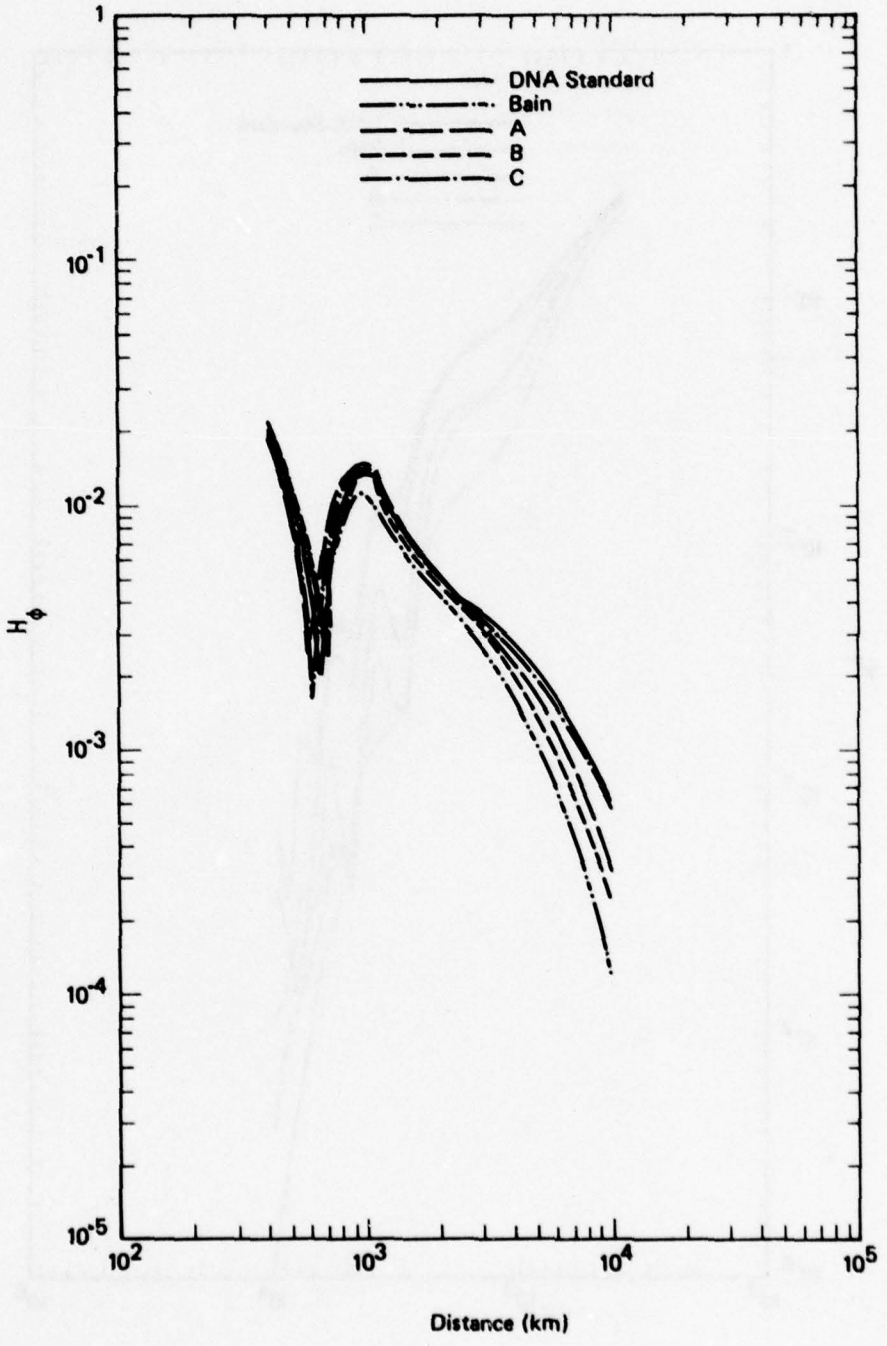

Fig. 5--Magnetic intensity versus distance; 20 kHz

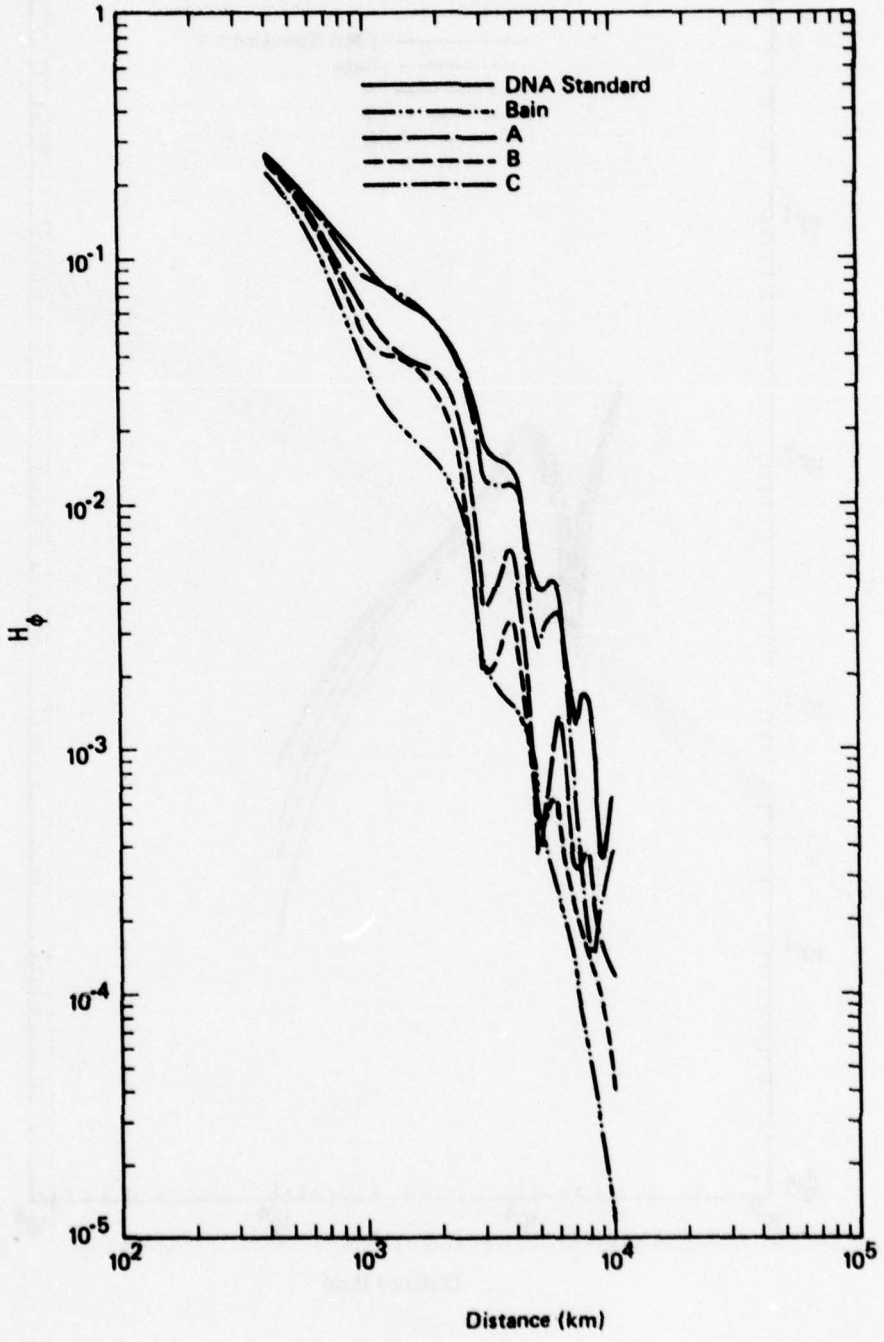

Fig. 6--Magnetic intensity versus distance; 35 kHz

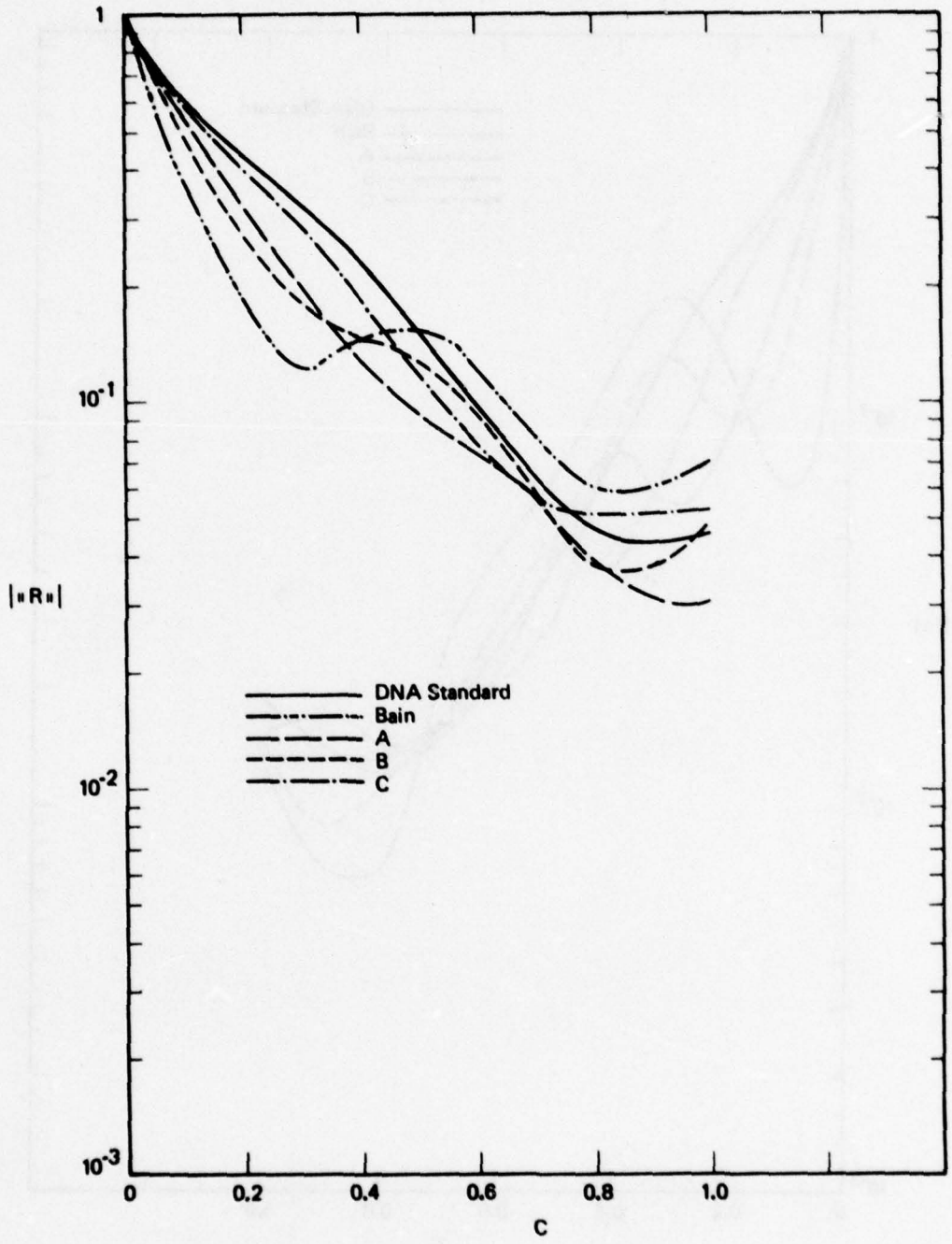

Fig. 7--Reflection coefficient versus cosine of incidence angle; 20 kHz

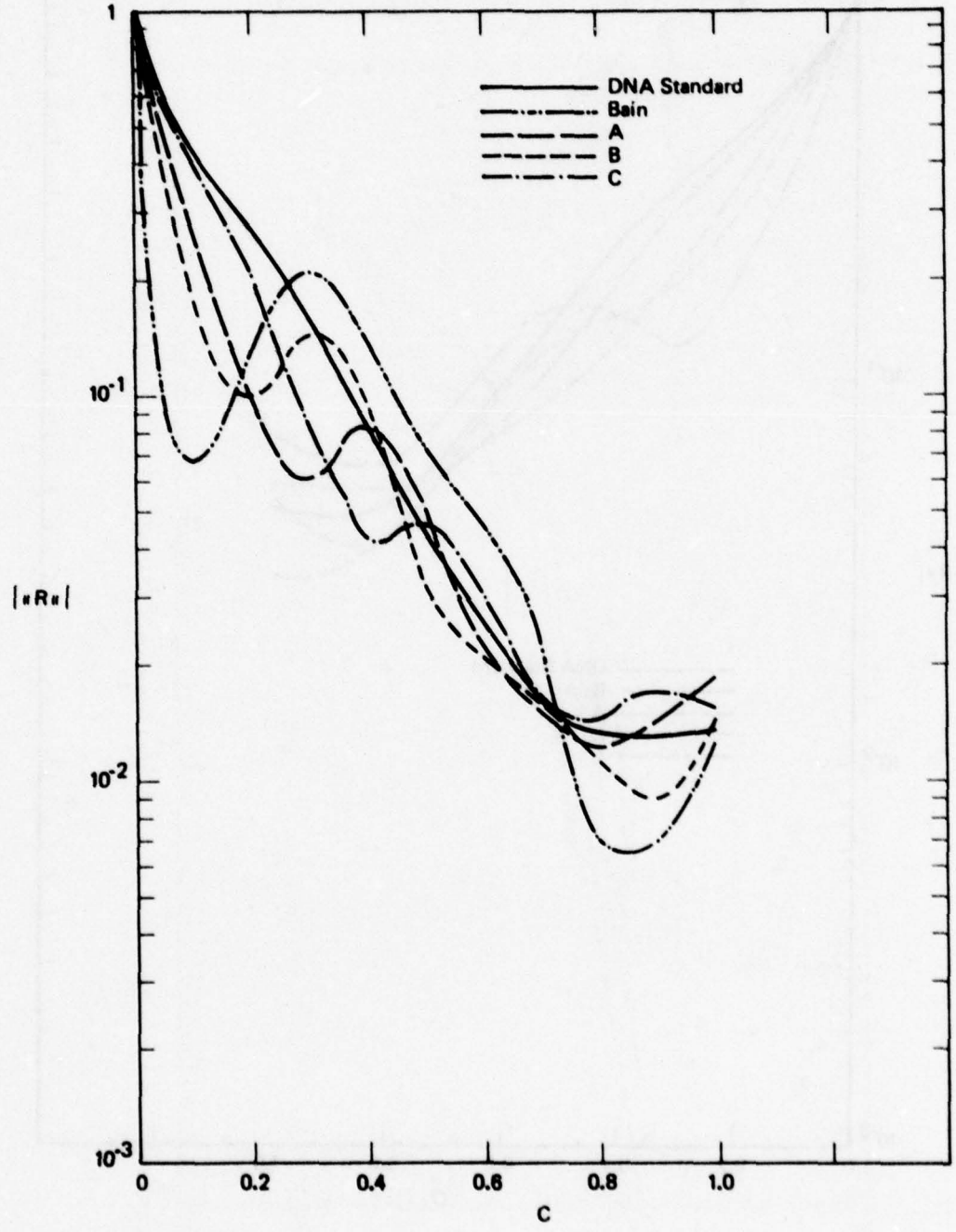

Fig. 8--Reflection coefficient versus cosine of incidence angle; 35 kHz

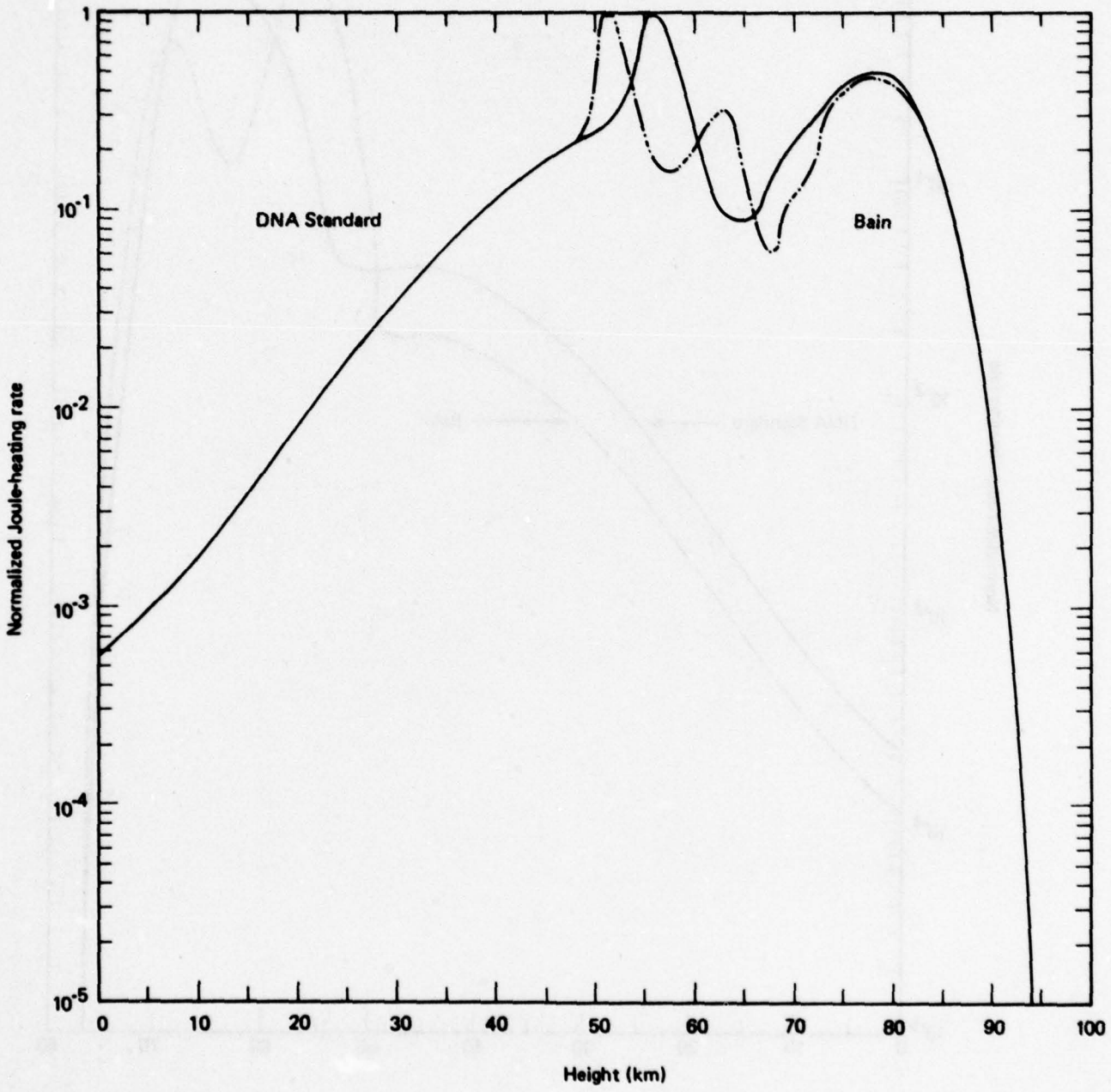

Fig. 9--Normalized Joule-heating height-profiles; 75 Hz

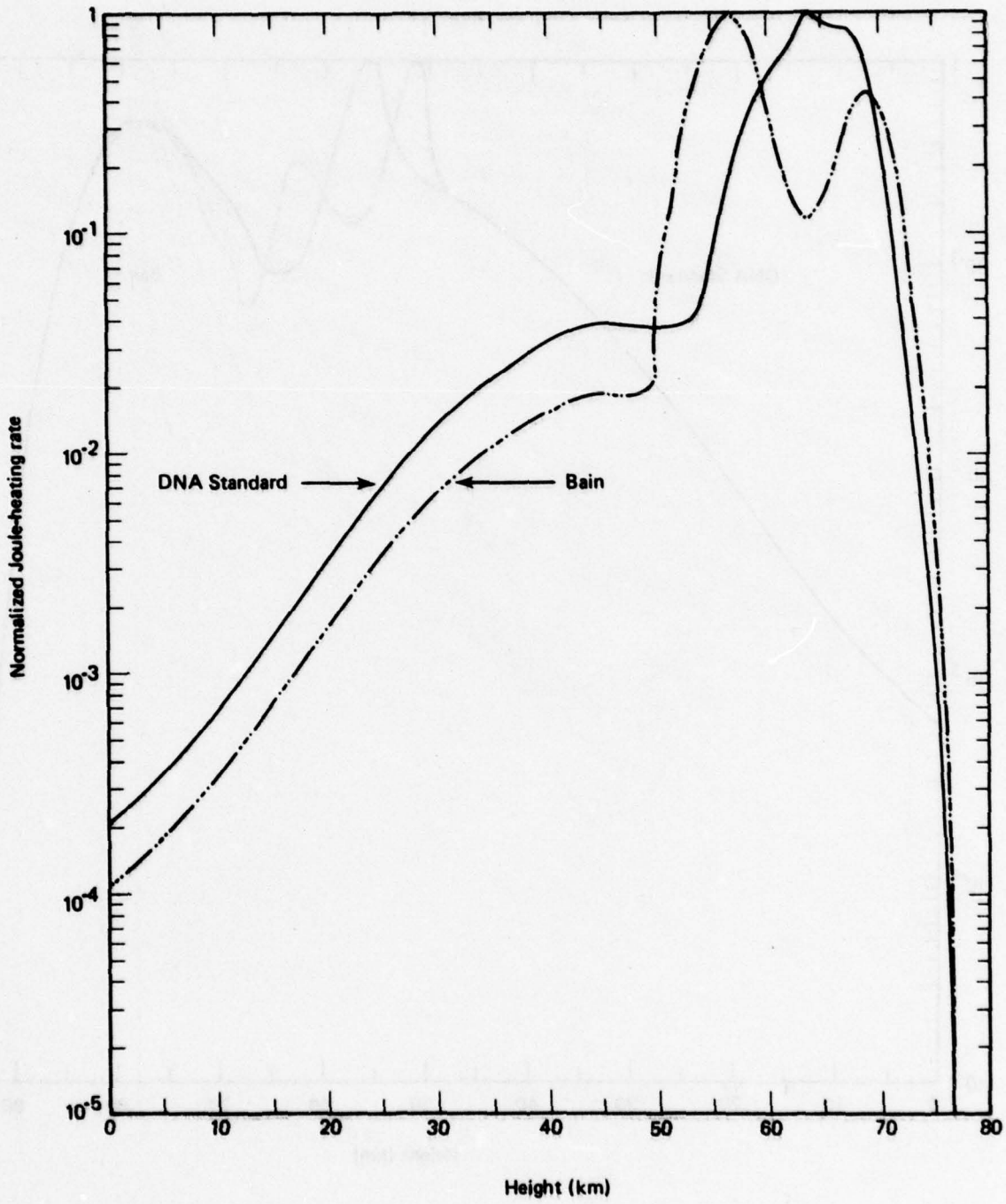

Fig. 10--Normalized Joule-heating height-profiles; 20 kHz

should be compared because all profiles have been normalized to have a peak value of unity. The heating profiles above about 70 km are less accurate than at lower altitudes because of the omission of the geomagnetic field in the calculations.

DISCUSSION

The results in Table 1 for 45 Hz and 75 Hz show that the effects of the C-layer ledge on ELF propagation are small. Only slight differences in attenuation rate, η, and excitation factor, A, are noted among the different models considered. Moreover, no clear trend is evident--Model B giving the lowest attenuation at 45 Hz and Model C the lowest attenuation at 75 Hz. Figures 3 and 4 give the ELF field-strength versus distances for these frequencies, and again indicate only minute differences for the various ionospheric models used. Even at a propagation distance of 10 Mm, the spread in calculated field strength is only about 35 percent (2 dB).

The results for VLF/LF are very different than those described above at ELF. Table 1 shows that at 20 kHz, significant differences in calculated attenuation rates occur among the various models. Even larger differences in η are shown at LF (35 kHz). However, no important dependence of the excitation factor on the C-layer ledge is noted.

The trend in the results for VLF/LF is much more regular than at ELF. In every instance, the standard DNA model gives the lowest attenuation rate, indicating that the effect of the C-layer ledge assumed here is to degrade the propagation. For all cases, the Bain model of the C-layer ledge gives the highest attenuation rate.

The results for Models A, B, and C are of interest because they illustrate the dependence of propagation on the altitude of the layer--the electron density and thickness having been held constant for these three models. For all cases, the lowest-altitude model (B) gives the highest attenuation whereas the highest-altitude model (C) gives attenuation rates only slightly greater than does the standard model. Two competing effects occur when the altitude of the layer is changed. First, because of the decrease of collision frequency with altitude, a given electron density corresponds to a greater refractive index at say, 61 km than at 55 km. Second, and conversely, a 100 el/cm^3 increase in electron density is a relatively modest addition to the standard density at 61 km, but is a very large relative enhancement at 55 km. For the models assumed, the second effect is clearly dominant because the ledge centered at 55 km caused the greatest increase in attenuation rate. Of course, this trend of the effect of the ledge increasing as its altitude is decreased would not continue indefinitely. Placing the ledge at *too* low an altitude (e.g., 40 km) would have virtually no effect on propagation, because the electron mobility would be destroyed by the large collision frequency.

Figures 5 and 6 show that the effects of a C-layer ledge on VLF/LF field strength can be considerable, provided that the ledge exists over lateral distances of many megameters. At 20 kHz, Fig. 5 shows that the spread among the calculated fields is about a factor of four, which corresponds to 12 dB. At 35 kHz, Fig. 6 shows spreads of up to a factor of 40, which corresponds to about 30 dB.

Figures 7 and 8 provide insight into the behavior of the waveguide modes given above. Note that the full-wave mode calculations indicate

that the eigen-cosine of the lowest VLF/LF modes are about 0.2 at 20 kHz and 0.15 at 35 kHz. These eigen-cosines correspond physically to the cosine of the incidence angle at the ionosphere. For C = 0.2, Fig. 7 shows that the ordering of $|_{\uparrow\uparrow}R_{\downarrow\uparrow}|$ for the various models at 20 kHz is the same as the ordering of η in Table 1; i.e., the reflection coefficient is lowest (η highest) for the Bain model, and so forth. Similar conclusions are drawn from Fig. 8 for 35 kHz and C = 0.15.

An important conclusion drawn from Figs. 7 and 8 is that the relative effects of the various assumed C-layer ledges depend strongly on incidence angle. For example, as discussed above, the Bain model gives the lowest reflection coefficient for long propagation paths, which correspond at oblique incidence ($C \lesssim 0.2$). For steeper incidence angles ($C \approx 0.6$; $\theta = 53°$), however, the Bain model gives the *highest* reflection coefficient of any of the models considered.

Figure 9 indicates why the C-layer ledge has such a small influence on ELF propagation. As shown by the Joule-heating profile, the important ionospheric interactions occur over a broad range of altitudes that extend from about 50 km to 85 km at 75 kHz. Only the lowest 10 km or so of this range is significantly affected by the Bain model of the C-layer ledge. Moreover, the enhanced heating between 50 km to 55 km is largely compensated by reduced heating between 55 km to 60 km, causing the attenuation rate--which is essentially proportional to the area under the heating profile--to be relatively unaffected.

Conversely, at 20 kHz, Fig. 10 shows that for the standard model the heating peak occurs in a well-defined region about 15-km thick, centered

at about 65 km. The main effect of the Bain C-layer is to lower this heating region--and, presumably, the reflection height--by nearly 10 km. Although not evident from the normalized curves shown in Fig. 10, the heating peak--and the area under the heating curve--for the Bain model is about twice as large as for the standard model.

III. RELATIONSHIPS AMONG INCIDENCE ANGLE, FREQUENCY, AND VLF/LF REFLECTION HEIGHTS

The range of altitudes from which VLF/LF signals are reflected from the ionosphere depends on the incidence angle and frequency of the wave. Ordinarily, the reflection height-range tends to be lowered if 1) the wave frequency is reduced, or 2) if the incidence angle is made more oblique. Thus, for a given frequency, long-path signals tend to interact with lower ionospheric heights than do short-path signals, which have steep incidence angles. For the reasons stated above, however, it should be possible to cause oblique waves to interact with the same ionospheric regions as steep-incidence waves by properly adjusting the frequency. Accordingly, this section analyzes the relationship between incidence angle and frequency of VLF/LF waves that reflect from a given ionospheric height-range.

BACKGROUND

Some progress on the above problem has already been reported in the literature. Booker and Crain (*1964*) computed reflection loss by assuming (on intuitive grounds without proof) that VLF/LF reflection takes place near a level where

$$2\omega\cos^2\theta = \omega_p^2/\nu_e \equiv \omega_0 \quad . \tag{3}$$

In Eq. (3), ω is the angular frequency of the wave, θ is the incidence angle at the ionosphere, ν_e is the electron-collision frequency, and ω_p^2 is the electron-plasma frequency, which depends linearly on the electron

density, N_e. Thus, the characteristic frequency, ω_0, depends on height through the ratio, N_e/ν_e; and Eq. (3) states that two waves will sample the same height-range (i.e., the same values of N_e/ν_e) provided that the product $\omega\cos^2\theta$ is kept constant.

Because Booker and Crain simply wrote down--rather than derived--Eq. (3), they give no criteria for its validity or range of applicability. Of course, given the absence of the gyrofrequency in Eq. (3), the applicability is clearly limited to daytime or disturbed conditions where geomagnetic effects play a relatively minor role. Equation (3) was put on a more rigorous footing by Field and Engle (*1965*), who show that provided

$$\cos^2\theta \ll 1 \quad , \tag{4a}$$

and

$$\omega_0 \propto e^{\beta Z} \quad , \tag{4b}$$

the main reflections occur in a several-kilometer altitude range centered near the altitude where

$$\sqrt{2}\ \omega\cos^2\theta = \omega_0 \quad , \tag{5}$$

which is essentially the same as Eq. (3), and--like Eq. (3)--is invarient to changes in ω or $\cos\theta$ provided the product $\omega\cos^2\theta$ remains constant.

DERIVATIONS

The task at hand is to derive relations analogous to Eqs. (3) or (5) that are not restricted by the conditions (4a, 4b) and that apply under conditions in which the geomagnetic field must be included. The approach taken is to derive expressions for the ionospheric reflectivity-per-unit-

height, $\tilde{R}(z)$, and determine which, if any, combinations of ω and $\cos\theta$ will leave $\tilde{R}$ unchanged. Only partial success is achieved because, although a useful relation unrestricted by conditions 4a, 4b is found, the equations for conditions where the geomagnetic field must be included are too complicated to be of practical value.

Vertical Polarization

We begin by defining the following three quantities that occur throughout the derivation:

$$n^2 \approx 1 + i\frac{\omega_0}{\omega} \quad , \tag{6}$$

$$q^2 \approx \cos^2\theta + i\frac{\omega_0}{\omega} \quad , \tag{7}$$

$$Q = q/n^2 \quad .$$

In the above expressions, ω_0, which is a function of height, is defined by Eq. (3), n^2 is the ionospheric refractive index, and q is the solution to the well-known Booker quartic. Equations (6) and (7) are based on the approximation that

$$\nu_e > \omega_c \text{ and } \omega \quad ,$$

which is valid below 70 km or so for VLF/LF.

The exact, full-wave equation for the reflection coefficient is nonlinear and, hence, must be solved numerically. Because an analytic relation between ω and $\cos\theta$ is desired, some approximations must be made. Specifically, attention is restricted to conditions where the reflectivity-per-unit-height is not too large.

For vertical polarization, the relevant Maxwell equations are

$$\frac{dE}{dz} = -ikqQH \tag{9}$$

and

$$\frac{dH}{dz} = -ikn^2E \quad , \tag{10}$$

where k is the free-space number, E is the horizontal electric field, and H is the normalized horizontal magnetic intensity* (*Budden, 1961, p. 142*). The method of solution is based upon deriving correction terms to the WKB approximation, which neglects reflections altogether. Thus, we insert

$$E_{u,d} \approx \pm QH_{u,d} \tag{11}$$

into Eqs. (9) and (10), where the subscripts u,d denote upgoing and downgoing waves, respectively. After some rearrangement, the following coupled equations for the upgoing and downgoing waves are obtained:

$$H_u' + \left[\frac{Q'}{2Q} + ikq\right] H_u = \frac{Q'}{2Q} H_d \tag{12a}$$

$$H_d' + \left[\frac{Q'}{2Q} - ikq\right] H_d = \frac{Q'}{2Q} H_u \quad , \tag{12b}$$

where the prime denotes z-differentiation. The quantity Q'/2Q represents coupling between upgoing and downgoing waves, and is treated as a perturbation term.

The zero-order solution to Eq. (12a), obtained by neglecting the right-hand side, is easily shown to be

---

*Specifically, H differs from the unnormalized magnetic intensity by a factor of 120π ohms.

$$H_u = \frac{H_i \cos\theta}{\sqrt{Q}} \exp\left[-ik \int_0^z q(\zeta)\, d\zeta\right] \quad , \tag{13}$$

where H_i is the wave incident on the ionosphere from below; i.e., $H_u = H_i$ at $z = 0$. Equation (13) is the well-known WKB representation of an upgoing, vertically polarized wave.

The downgoing wave generated by the upgoing wave is calculated to first order by inserting Eq. (13) into the right-hand side of Eq. (12b):

$$H_d' + \left[\frac{Q'}{2Q} - ikq\right] H_d = \left[\frac{Q'}{2Q}\right] \frac{H_i \cos\theta}{\sqrt{Q}} \exp\left[-ik \int_0^z q(\zeta)\, d\zeta\right] \quad . \tag{14}$$

Equation (14) is a linear, first-order, differential equation that may be integrated immediately. The resulting expression for H_d, subject to the physically necessary condition that $H_d = 0$ at $z = \infty$, is

$$H_d(z) = \int_z^\infty \left\{\frac{H_i \cos\theta}{\sqrt{Q(\zeta)}} \exp\left[-ik \int_0^\zeta q\, d\eta\right]\right\} \left\{\sqrt{\frac{Q(\zeta)}{Q(z)}} \exp\left[-ik \int_z^\zeta q\, d\eta\right]\right\} \cdot \left\{\frac{Q'(\zeta)\, d\zeta}{2Q(\zeta)}\right\} \quad . \tag{15}$$

The reflection coefficient at the ground, R_v, is obtained by setting $z = 0$ in Eq. (15), and noting that $H_d(0) = RH_i$, and $Q(0) = \cos\theta$, whence

$$R_v = -\int_0^\infty d\zeta \left[\frac{Q'}{2Q}\right] \exp\left[-2ik \int_0^\zeta q\, d\zeta\right] \quad , \tag{16}$$

which is a well-known result for weakly reflecting media derived in a different manner by Wait (*1970*).

The terms in Eq. (15) are grouped to permit a clear physical interpretation. The first curly brackets contain the expression for the upgoing wave at a height, ζ; the second curly brackets, the expression for the reduction in strength of a downgoing wave in propagating from a height ζ to a lower height, z. Thus, the quantity in the third bracket denotes the amount of upgoing wave converted into downgoing wave in the thin layer extending from ζ to $\zeta + d\zeta$. A similar interpretation can be obtained from Eq. (16) by noting that the exponential factor in the integrand accounts for the loss suffered by an upgoing wave propagating to the height, ζ; and the loss suffered by a downgoing wave propagating from the height, ζ, back down to the ground at $\zeta = 0$. Thus, the reflectivity-per-unit-height, $\tilde{R}_v$, can be written, by using Eqs. (6) through (8),

$$\tilde{R}_v = \frac{-Q'}{2Q} = \frac{-i\omega_0'}{2(\omega\cos^2\theta + i\omega_0)} \left[\frac{\omega - i\omega_0 - 2\omega\cos^2\theta}{\omega + i\omega_0}\right] , \qquad (17)$$

which has the following magnitude:

$$|R_v| = \frac{\omega_0'}{2\left[\omega^2\cos^4\theta + \omega_0^2\right]^{1/2}} \left[1 - \frac{2\omega^2 \sin^2 2\theta}{\omega^2 + \omega_0^2}\right]^{1/2} . \qquad (18)$$

Horizontal Polarization

The derivation for horizontal polarization proceeds exactly as described above for vertical polarization, except that the electric field is used rather than H. Without going into details, note that, aside from unimportant multiplicative factors, the equations for horizontal polarization are identical to those for vertical polarization, except that the

quantity, Q, is replaced by the simpler quantity, q. The reflection coefficient is

$$R_h = \int_0^{\infty} d\zeta \left[\frac{q'}{2q}\right] \exp\left[-2ik \int_0^{\zeta} q\, d\eta\right] \quad ; \tag{19}$$

and the reflectivity-per-unit height is given by

$$\tilde{R}_h = \left[\frac{q'}{2q}\right] = \frac{i\omega_0'}{2\left[\omega\cos^2\theta + i\omega_0\right]} \quad , \tag{20}$$

which has the magnitude

$$|\tilde{R}_h| = \frac{\omega_0'}{2\left[\omega^2\cos^4\theta + \omega_0^2\right]^{\frac{1}{2}}} \quad . \tag{21}$$

DISCUSSION

Subject to the approximations made in the derivations, $\tilde{R}_v$ and $\tilde{R}_h$ determine the heights at which reflection occurs. Of course, as indicated by Eqs. (16) and (19), $\tilde{R}_v$ and $\tilde{R}_h$ do not completely determine the ground-level reflection coefficients, which also depend on the exponential term accounting for losses suffered propagating to and from the reflection regions. Thus, the following subtle distinction arises. If one wishes to obtain the same reflection coefficient for obliquely and steeply incident waves, then ω and $\cos\theta$ must be adjusted such that the entire integrand of Eqs. (16) or (19) remains constant. However, if the goal is to use an obliquely and a steeply incident wave to sample the same ionospheric height ranges, then ω and $\cos\theta$ must be adjusted in a way that $\tilde{R}_v$ and $\tilde{R}_h$ remain unchanged. In the latter case, the ground-level coefficients will not necessarily be the same.

In principle, $\tilde{R}_v$ and $\tilde{R}_h$ account for both gradient reflection, characterized by large values of ω_0', and classical-turning-point reflection, characterizied by either q or $Q \approx 0$. Because of the complex functional forms used to approximate q or Q (see Eqs. (7) and (8)), neither q or Q can vanish in the altitude range considered here, and only gradient reflection is a factor.

In Eqs. (17), (18), (20), and (21), the height dependences of $\tilde{R}_v$ and $\tilde{R}_h$ are contained solely in ω_0, and its derivative, ω_0', whereas the dependence on ω and $\cos\theta$ is shown explicitly. The question to be answered is whether a simple functional relationship can be found whereby ω and $\cos\theta$ can be varied without altering $\tilde{R}_v$ or $\tilde{R}_h$. The answer is remarkably simple for horizontal polarization because, as shown by Eq. (20), *$\tilde{R}_h$ depends on frequency and incidence angle solely through the combination $\omega\cos^2\theta$*. Thus, for horizontal polarization, the conclusion that the reflectivity-per-unit-height is invarient to changes in ω or $\cos\theta$, provided that $\omega\cos^2\theta$ remains constant, applies even when the conditions (4a) and (4b) are violated. Of course, this conclusion is not totally unqualified, because the derivation is based upon the assumption that the medium changes slowly enough that the product of $\tilde{R}_h$ and the local inverse vertical wave number, $(kq)^{-1}$, is less than unity; i.e., the condition

$$\left|\frac{q'}{2kq^2}\right| < 1 \qquad (22)$$

must hold. Of course, Eq. (22) is the validity criterion for the WKB approximation, and Field and Engle (*1964*) derived Eq. (5) simply by maximizing the left-hand side of Eq. (22).

The situation is more complicated for vertical polarization because, as shown by Eq. (17), $\tilde{R}_v$ depends on ω and $\cos\theta$ through factors other than $\omega\cos^2\theta$. For either oblique or steep incidence, however, approximate forms for $\tilde{R}_v$ result, from which relatively simple conclusions can be drawn. For sufficiently oblique angles, Eq. (17) becomes

$$\tilde{R}_v \approx \frac{i\omega_0'}{2(\omega\cos^2\theta + i\omega_0)} \left[\frac{\omega - i\omega_0}{\omega + i\omega_0}\right] \quad \text{if} \quad \cos^2\theta << \tfrac{1}{2} \quad ; \tag{23}$$

whereas, for sufficiently steep angles, Eq. (17) becomes

$$\tilde{R}_v \approx \frac{i\omega_0'}{2(\omega\cos^2\theta + i\omega_0)} \quad \text{if} \quad \sin^2\theta << \tfrac{1}{2} \quad , \tag{24}$$

which is identical with Eq. (20) because the distinction between vertical and horizontal polarization disappears for nearly normal incidence. Both Eq. (23) and Eq. (24) depend only on the combination $\omega\cos^2\theta$. Further note that the magnitude of $\tilde{R}_v$ for oblique and steep incidence, as described by Eqs. (23) and (24), is identical* although the phases are different.

We thus conclude that steeply and obliquely incident, vertically polarized signals are reflected from about the same ionospheric heights provided that $\omega\cos^2\theta$ is held constant. This conclusion should be reasonably accurate, provided $\cos^2\theta << \frac{1}{2}$ or $\sin^2\theta << \frac{1}{2}$; i.e., for incidence angles greater than about 70° or less than about 20°. For intermediate angles and vertical polarization, no such relationship exists, as can be seen from Eq. (18).

---

*This conclusion also follows from Eq. (18), with $\theta \approx 0$ or $\theta \approx \pi/2$.

This section has been concerned with ionospheric conductivity height-profiles essentially devoid of rapid transition regions, which, because of large height-derivatives, cause validity criteria such as Eq. (22) to be violated. It is precisely at such "ledges," however, that waves are reflected regardless of frequency and incidence angle (aside from the Brewster angle). Thus, in the approximation opposite to that used here--the nearly sharply bounded layer--both steeply and obliquely incident waves will reflect from the same height regardless of frequency, provided only that the wave can penetrate to and from the layer.

We were not able to derive useful relations between ω and $\cos\theta$ for situations in which the geomagnetic field must be included. Aside from very special conditions in which the propagation is essentially isotropic (e.g., east-west propagation at the equator, normally incident circularly polarized waves at the geomagnetic poles), the equation for reflectivity-per-unit-height becomes much too complicated to be of practical analytic value.

REFERENCES

Alpert, Y. L., *Radio Wave Propagation and the Ionosphere, Vol. 1 The Ionopshere*, Consultants Bureau, New York-London, 1973.

Bain, W. C., "The Use of VLF Propagation in Ionospheric Modelling," *ELF-VLF Radio Wave Propagation*, Proc. of NATO Adv. Study Inst., D. Reidel Publishing Co., 1974.

Budden, K. G., *Radio Waves in the Ionosphere*, Cambridge University Press, Cambridge, England, 1961.

Crain, C. M., and H. G. Booker, "The Effects of Ions on Low Frequency and Very Low Frequency Propagation in an Abnormally Ionizied Atmosphere," *J. Geophys. Res.*, Vol. 69, November 1964, pp. 4713-4716.

Field, E. C., and R. D. Engel, "The Detection of Daytime Nuclear Bursts Below 150 km by Prompt VLF Phase Anomalies," *Proc. IEEE Vol. 53*, December 1965, pp. 2009-2010.

Field, E. C., M. Lewinstein, and M. A. Dore, *Effects of Antenna Elevation and Inclination on VLF/LF Signal Structure*, Pacific-Sierra Research Corp., Report RADC-TR-76-375, December 1976.

Krasnushkin, P. Ye., and N. Federov, "Determination of the Electron Density Profile of the Lower Ionosphere From Surface Wave Fields with Allowance for a Possible Ionization Valley," *Geomagnetism and Aeronomy, Vol. VI, No. 6*, 1966, p. 839.

Knapp, W. S., and K. Schwartz, *Aids for the Study of Electromagnetic Blackout*, General Electric/TEMPO, DNA 3499, 1 Febraury 1975.

Risbeth, H., and O. K. Garriot, *Introduction to Ionospheric Physics*, Academic Press, New York, 1969.

Wait, J. R., *Electromagnetic Waves in Stratified Media*, Pergamon Press, New York, 1970.